

## Article

# Characteristics of Hybrid Nanolubricants for MQL Cooling Lubrication Machining Application

Syh Kai Lim <sup>1</sup> , Wan Hamzah Azmi <sup>2</sup>, Ahmad Shahir Jamaludin <sup>1</sup> and Ahmad Razlan Yusoff <sup>1,3,\*</sup> 

<sup>1</sup> Faculty of Manufacturing and Mechatronic Engineering Technology, Universiti Malaysia Pahang, Pekan 26600, Pahang, Malaysia

<sup>2</sup> Faculty of Mechanical and Automotive Engineering Technology, Universiti Malaysia Pahang, Pekan 26600, Pahang, Malaysia

<sup>3</sup> Centre for Advanced Industrial Technology, Universiti Malaysia Pahang, Pekan 26600, Pahang, Malaysia

\* Correspondence: razlan@ump.edu.my

**Abstract:** Efficient and effective lubricants have great application prospects in the manufacturing industries. Minimum quantity lubrication (MQL) machining with low flow rate of nanolubricants is investigated for cooling and lubrication during the process. This paper investigates the characterization of graphene-mixed aluminium oxide (G-Al<sub>2</sub>O<sub>3</sub>) hybrid nanomixture spent lubricants for MQL machining purposes. The main advantage of this method is to reduce the disposal lubricants to develop high-performance cooling-lubrication by using nanolubricants of G-Al<sub>2</sub>O<sub>3</sub> nanoparticles in different volume composition ratios at a constant 1.0% volume concentration in a base liquid mixture of 40% spent lubricants. Before conducting the measurements of the nanolubricants' thermal conductivity and dynamic viscosity, the nanolubricants were homogenous and stable. The tribological performance of all ratios was evaluated by using a four-ball wear tribotester machine. The thermal conductivity peak value for the G-Al<sub>2</sub>O<sub>3</sub> hybrid nanolubricant was obtained and the highest enhancement, up to 29% higher than the base liquid solution, was obtained. The dynamic viscosity variation for all ratios was lower than the 40:60 ratio. The properties enhancement ratio suggests that G-Al<sub>2</sub>O<sub>3</sub> hybrid nanolubricants with 1.0% volume concentration aid in the heat transfer, especially for ratios of 60:40 and 20:80. The lowest coefficient of friction (COF) for a ratio of 60:40 was obtained to be 0.064, with 45% enhancement as compared to the base liquid solution. In conclusion, optimum ratios for G-Al<sub>2</sub>O<sub>3</sub> hybrid nanolubricants were determined to be 20:80 and 60:40. Regarding the properties enhancement ratio, the combination of enhanced thermophysical and tribological properties had more advantages for cooling lubrication application.

**Keywords:** spent lubricant; four-ball wear test; thermal conductivity; dynamic viscosity; G-Al<sub>2</sub>O<sub>3</sub> hybrid nanolubricants



**Citation:** Lim, S.K.; Azmi, W.H.; Jamaludin, A.S.; Yusoff, A.R. Characteristics of Hybrid Nanolubricants for MQL Cooling Lubrication Machining Application. *Lubricants* **2022**, *10*, 350. <https://doi.org/10.3390/lubricants10120350>

Received: 31 October 2022

Accepted: 24 November 2022

Published: 5 December 2022

**Publisher's Note:** MDPI stays neutral with regard to jurisdictional claims in published maps and institutional affiliations.



**Copyright:** © 2022 by the authors. Licensee MDPI, Basel, Switzerland. This article is an open access article distributed under the terms and conditions of the Creative Commons Attribution (CC BY) license (<https://creativecommons.org/licenses/by/4.0/>).

## 1. Introduction

The use of lubricants in manufacturing industry is inevitable, which contributes between 10 and 17% of the total machining cost [1], while the increment of at least 1.2% of the total world consumption of lubricants with 38 million tons of oil equivalent will be consumed over the next decade [2]. For example, the European Union alone has been consuming about 320 million tons of lubricant in recent years, and 85% of lubricants ended up as total loss applications [3]. Hence, recycling spent lubricants with better cooling lubrication and heat transfer performance is crucial in the machining process system. A variation in the type of nanomixtures and approaches to improve the heat transfer performances was investigated by researchers [4–7]. Some investigation research related to engineering fields, such as a cooling–lubrication system and heat exchanger, showed that nanomixtures are capable of enhancing the heat transfer characteristics of industrial tools [8–10]. Nanomixtures considering stable conditions for nanoparticles suspension

with sizes no larger than 150 nm are randomly dispersed in a base liquid [11]. Only in recent years has the investigation of hybrid nanomixtures been more focused on the tribological characteristics and thermophysical properties in terms of dynamic viscosity and thermal conductivity [12–16]. Akilu et al. [17] revealed that the hybrid nanomixtures were considered as a combination of several types of nanoparticles suspended in a heat transfer liquid to achieve a homogeneous stable liquid solution.

Dynamic viscosity is an important parameter that affects the coefficient of heat transfer and heat dissipation performance [18]. A study by Ho et al. [19] found that the MEPCM–Al<sub>2</sub>O<sub>3</sub> nanomixtures showed enhancement with the increase in volume concentration of the nanoparticles suspended in base solution. Esfe et al. [20] investigated a hybrid nanomixture with water-based Ag–MgO composites nanoparticles, and they found that the dynamic viscosity increased with the increase in nanoparticles concentration. Bahrami et al. [14] used Fe–CuO hybrid nanoparticles base ethylene glycol–water with a volume ratio of 80:20 to study rheological behavior. They measured for a concentration volume of 0.05–1.50% and temperature of 30–50 °C. The results indicated that nanomixtures in low-volume concentrations of nanoparticles performed as a Newtonian fluid, but the shear thinning situation occurred in higher nanoparticle volume concentrations and behaved non-Newtonian. Soltani et al. [21] also measured the dynamic viscosity of MgO–MWCNT nanomixtures with volume concentration ranges of 0.1–1.0%. They studied the dynamic viscosity in the temperature range of 30–60 °C and found that the nanomixtures exhibited Newtonian fluid behavior. The effect of experimental temperature was investigated and was found to be more significant for nanomixtures at higher concentrations.

The thermal conductivity enhancement is contributed to by a few factors, such as temperature, nanoparticle volume concentration and size, and the stability of nanomixtures. An investigation by Baghbanzadeh et al. [22] measured hybrid SiO<sub>2</sub>–MWCNT nanomixtures, showing thermal conductivity enhancement with the increment in nanoparticles concentration, while the thermal conductivity of the nanomixture in a high nanoparticle volume concentration was found to have a minimum enhancement. The bigger percentages of MWCNT in the hybrid nanomixtures provided a better effect in thermal conductivity as compared to SiO<sub>2</sub> nanoparticles. Another study by Jana et al. [23] investigating the volume concentration of 1.4% AuNP nanomixtures showed a thermal conductivity enhancement up to 37% compared to water. Suresh et al. [24] evaluated the thermal conductivity of Al<sub>2</sub>O<sub>3</sub>–Cu suspended in water based nanomixtures and found the effect of thermal conductivity augmentation to be approximately 12% with the increase in the nanoparticle concentrations. An investigation by Kumar et al. [25] measured Zn–Cu nanoparticles in various base liquids, such as paraffin oil, plant oil, and SAE oil. Their findings showed that the thermal conductivity of Zn–Cu in plant oil provided a maximum enhancement of 53% as compared with the others. Another study of MEPCM–Al<sub>2</sub>O<sub>3</sub> nanomixtures in thermal conductivity was performed by Ho et al. [19]. They reported that the thermal conductivity increased by approximately 4% with the nanoparticle volume concentration.

Nanolubricants for tribological properties have recently attracted attention for scientific investigation and application. The significance of using hybrid nanoparticle compositions is that they exhibit better tribological properties than single-component nanoparticles [26]. Luo et al. [27] demonstrated the tribological properties of the lubricant hybrid TiO<sub>2</sub>–Al<sub>2</sub>O<sub>3</sub> nanoparticles using the friction test. The hybrid nanoparticles' stability in the lubricants base enhanced the friction coefficient with 0.1% concentration. Furthermore, it was found that the TiO<sub>2</sub>–Al<sub>2</sub>O<sub>3</sub> nanoparticles established better anti-friction properties as compared to pure TiO<sub>2</sub> or Al<sub>2</sub>O<sub>3</sub> nanoparticles. In another paper, Alimirzaloo et al. [28] used Al<sub>2</sub>O<sub>3</sub>–CuO hybrid nanoparticles in paraffin-based lubricants. They observed that the tribological properties significantly improved by 41% with a nanoparticles concentration of 0.8% as compared to conventional lubricants. Cheng and Qin [29] described the tribological properties of a graphene-based lubricant using the friction test and the results showed a 40–60% reduction in coefficient of friction. A similar study was conducted using graphene suspended in SAE20W-50 motor oil or ethylene glycol base liquid from another paper [30].

They evaluated that a reduction of 60–80% in wear rate and the minimum value of the friction coefficient was 0.057 with a 0.5% concentration of graphene nanoparticles.

Therefore, the need to investigate the thermo-physical properties and friction parameter of hybrid nanolubricants is essential. These are crucial to investigate the behavior and measure the factors affecting the hybrid nanolubricants properties which lead to the enhancement in heat dissipation and lubrication performances. Hybrid nanolubricants with graphene exhibited excellent friction performance and are capable of improving thermal conductivity. Cheng and Qin [29] investigated graphene-based grease for friction performance and found that it could reduce the friction coefficient up to 60%. Their result indicated that graphene adsorbs on the surface of metal and acts as protective coating. Hajjar et al. [30] concluded that graphene nanosolution dispersed in water without any surfactant showed a thermal conductivity enhancement of approximately 47% just by using ultrasonication. To the best of the authors' knowledge, the study on the effect of hybrid ratios for two types of nanoparticles suspended in mixture is limited in the literature. In the present study, the various hybrid ratios of G-Al<sub>2</sub>O<sub>3</sub> hybrid nanolubricants were carried out to emphasize the effect on thermo-physical properties and friction parameter with nanoparticle volume concentration at a level of ≤1.0%. Finally, optimum hybrid ratios are suggested by considering the enhancement ratio of G-Al<sub>2</sub>O<sub>3</sub> hybrid nanolubricants for application in a minimum quantity cooling lubrication (low flow rate) system in machining process.

## 2. Materials and Methods

### 2.1. Preparation of G-Al<sub>2</sub>O<sub>3</sub> Hybrid Nanolubricants

Two different types of nanoparticles were used in the preparation of nanolubricants. The nanolubricant was dispersing with nanoparticles of aluminum oxide (Al<sub>2</sub>O<sub>3</sub>) with average particle size of 13 nm; and graphene nanosheets with 5 nm thickness, were procured from Sigma-Aldrich Research Nanomaterials, Inc., Burlington, MA, USA. The present work studied the nanolubricants in base liquid mixture of spent lubricant to ethylene glycol (EG) in mixing volume ratio of 40:60 by directly synthesizing the graphene and Al<sub>2</sub>O<sub>3</sub> nanoparticles in a constant volume concentration of 1.0% with two-step preparation method. The experiments were conducted at four hybrid ratios nanoparticles (G-Al<sub>2</sub>O<sub>3</sub>) of 20:80, 40:60, 60:40 and 80:20. The characteristics of graphene, Al<sub>2</sub>O<sub>3</sub> nanoparticles and spent lubricant/EG mixture are presented in Table 1.

The spent lubricants were prepared in-house from recycling operation to remove the foreign contaminants, such as dirt and metal chips, while the EG was bought commercially. The recycling step involved solid particles filtration operation which could be accomplished through the application of filter paper and filter funnel to remove dirt and contaminated particles, as illustrated in Figure 1. The filter paper in sheet form was used to remove solid contaminants from the fluid. The mesh sizes of ordinary filter paper were 20 to 100 microns, depending on the particulate size produced during the manufacturing stage. A mesh finer than 20 microns can lead to product components being stripped from the fluid and should, therefore, be avoided [31]. Previous works of the present research group found that a base liquid composition ratio of 40:60 spent lubricant/EG mixture applicable as the cooling–lubrication medium [18] attained good heat transfer and reduced machining zone temperature. Equation (1) was used for dispersion of nanoparticles into base liquid mixture in volume concentration (%). The nanolubricant in 1.0% volume concentration was prepared as the first sample for both graphene and Al<sub>2</sub>O<sub>3</sub> nanolubricants with a 40:60 ratio (spent lubricant/EG). Then, the dilution process was conducted with the calculation by Equation (2), where  $V_1$  is known to synthesize the nanolubricant samples at several hybrid ratios in the volume concentration of 1.0%. The other research studies applied the same dilution method as presented in the literature [8,31,32].

$$\phi = \frac{m_p / \rho_p}{\frac{m_p}{\rho_p} + V_{bf}} \times 100 \quad (1)$$

$$\Delta V = (V_2 - V_1) = V_1 \left( \frac{\phi_1}{\phi_2} - 1 \right) \quad (2)$$

**Table 1.** Properties of graphene, Al<sub>2</sub>O<sub>3</sub> and spent lubricant/EG mixture.

Property	Graphene	Al <sub>2</sub> O <sub>3</sub>	Spent Lubricant/EG
Size, nm	-	13	-
Color	Black	White	Yellowish + White
Thickness, nm	5	-	-
Density, kg/m <sup>3</sup>	2200	4000	-

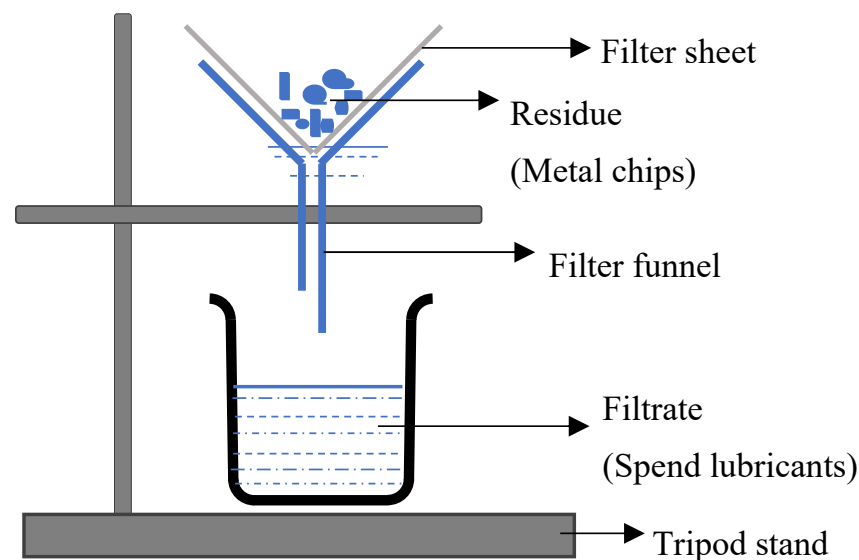


**Figure 1.** Physical recycling operation of spent lubricants.

The characterization of single Al<sub>2</sub>O<sub>3</sub> and graphene nanoparticles were undertaken, respectively, by field emission scanning electron microscopy (FESEM) and transmission electron microscopy (TEM) imaging techniques, which was also commonly utilized by other researchers [33,34]. Figure 2a presents the FESEM image for single Al<sub>2</sub>O<sub>3</sub> nanoparticles with magnifications of 300,000×. According to the FESEM images, the average diameter of single Al<sub>2</sub>O<sub>3</sub> nanoparticles is evaluated to be approximately 13 nm spherical size. TEM was utilized to evaluate the uniformity suspension of G-Al<sub>2</sub>O<sub>3</sub> nanoparticles in base liquid mixture, as shown in Figure 2b. The average Al<sub>2</sub>O<sub>3</sub> nanoparticle size dimension was much smaller as compared to the graphene nanoparticles. Hence, Al<sub>2</sub>O<sub>3</sub> nanoparticles could occupy space between the nanoparticles of graphene. Therefore, the two nanoparticles coordination and organization manner strongly depend on the hybrid ratios that describe the presence of each nanoparticle in the final solution. This phenomenon contributed to the reduction in space between the bigger nanoparticles, hence benefitting the thermal conductivity. Furthermore, the dynamic viscosity was predicted to be improved by different hybrid ratios. In order to investigate the different characteristics of the two hybrid nanoparticle distributions, the recent study evaluates the effect of the nanoparticles hybrid ratio on the relative dynamic viscosity, effective thermal conductivity and friction coefficient reduction of G-Al<sub>2</sub>O<sub>3</sub> hybrid nanolubricants.

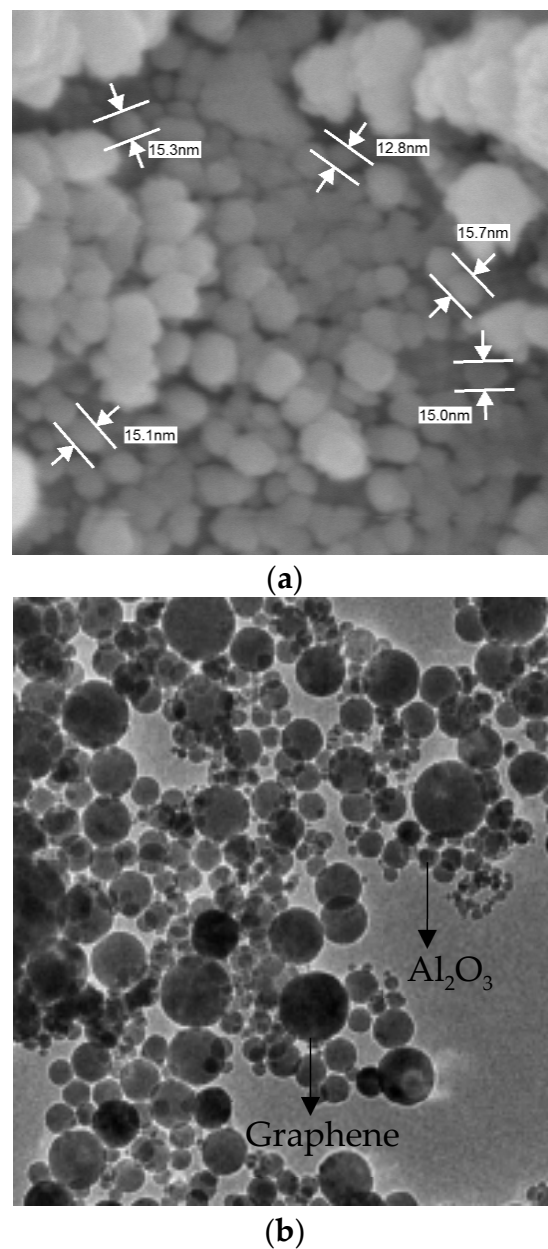


**Figure 2.** Images for single Al<sub>2</sub>O<sub>3</sub> nanoparticles and G-Al<sub>2</sub>O<sub>3</sub> hybrid nanolubricants. (a) FESEM result of dry Al<sub>2</sub>O<sub>3</sub> nanoparticles; (b) TEM image for G-Al<sub>2</sub>O<sub>3</sub> hybrid nanoparticles.

## 2.2. Stability of G-Al<sub>2</sub>O<sub>3</sub> Hybrid Nanolubricants

The hybrid nanolubricant was prepared by an ultra-sonication process to improve the stability of the nanoparticles suspension and reduce the nanoparticles agglomeration size [35]. A sample of 250 mL was subjected for ultrasonication for a certain time period to achieve good stability. According to Yu et al. [36], a nanomixture was determined to be homogenous and stable if the volume concentration or suspended nanoparticle size remained constant. Visual sedimentation was observed for each sample just after two weeks of preparation. The sedimentation observation for G-Al<sub>2</sub>O<sub>3</sub> hybrid nanolubricants is as shown in Figure 3a. Figure 3b shows that the G-Al<sub>2</sub>O<sub>3</sub> hybrid nanolubricants were observed to be stable after two weeks of preparation. The stability of hybrid nanolubricants was also evaluated using an ultraviolet–visible (UV–Vis) spectrophotometer. The absorption and the scattering of UV light were evaluated by comparing the penetrating light intensity of G-Al<sub>2</sub>O<sub>3</sub> hybrid nanolubricants with 40:60 (spent lubricant/EG) base liquid mixtures [37].



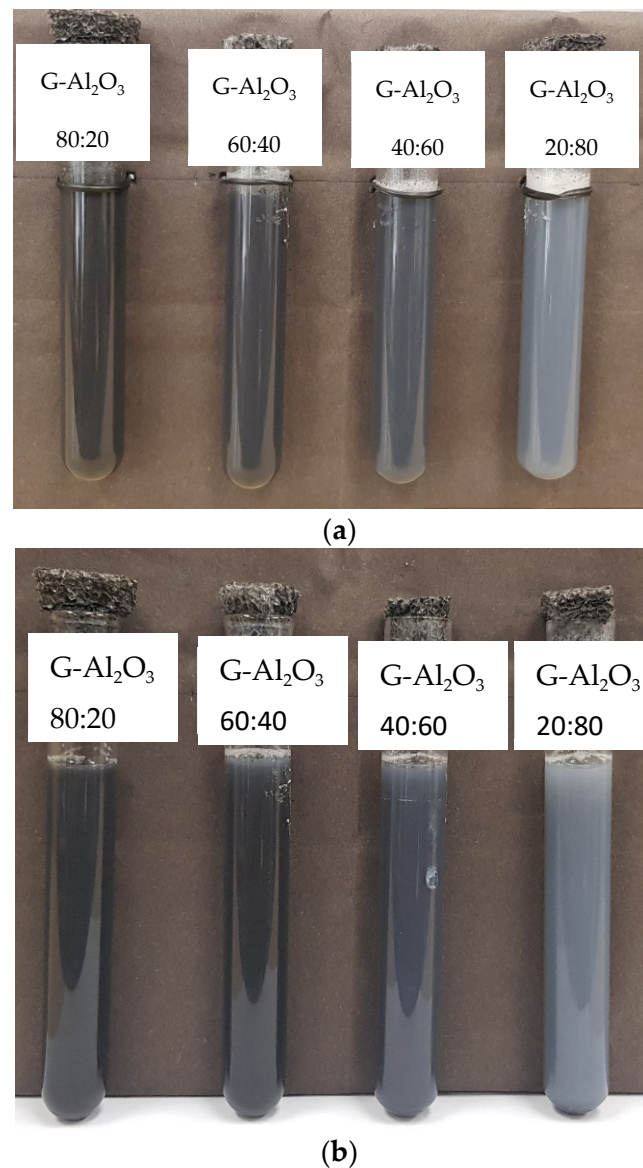


**Figure 3.** Four different hybrid ratios of G-Al<sub>2</sub>O<sub>3</sub> nanolubricants after two weeks of preparation for visual sedimentation. (a) First day; (b) after two weeks.

### 2.3. Thermal Conductivity Measurement

Thermal conductivity of G-Al<sub>2</sub>O<sub>3</sub> hybrid nanolubricants testing samples was measured through the KD2 Pro Property Analyzer (Decagon Devices), as illustrated in Figure 4. The experimental setup followed the standard of ASTM D5334. The thermal properties of liquid mixture were measured by the device for applying the transient line heat source. The thermal conductivity measurement was conducted in the temperature range from 30 to 80 °C. The water bath was used to maintain a constant temperature within an accuracy of 0.1 °C during the measurements. The KD2 Pro thermal sensor was validated with glycerin as the standard thermal conductivity verification liquid, which was delivered by manufacturer. A resulting value of 0.286 W/m·K within an accuracy of ±2% was attained. The thermal conductivity measurement was repeated three times within a 15 min interval time before the next reading for each data set, and the average value was considered. This is to minimize the measurement error of free convection with different temperatures along the sensor which is in direct contact with the hybrid nanolubricants testing samples [38].

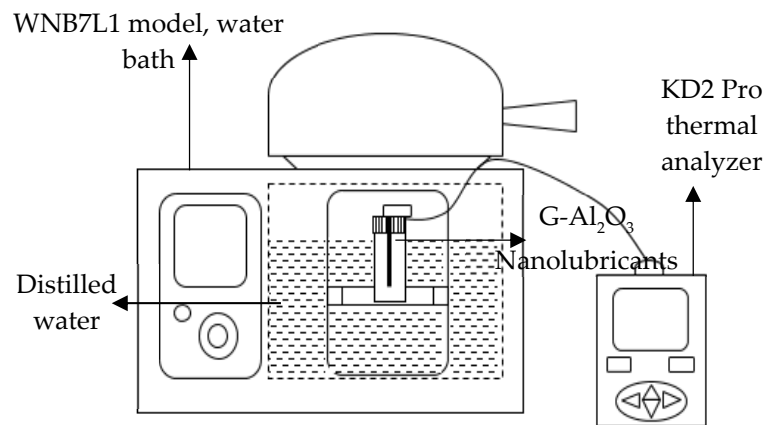


**Figure 4.** Schematic of the thermal conductivity measurement.

#### 2.4. Dynamic Viscosity Measurement

Dynamic viscosity of G-Al<sub>2</sub>O<sub>3</sub> hybrid nanolubricants samples were measured under the Brookfield Circulating Water Bath Ultra Programmable Rheometer as shown in Figure 5. The rheometer's applicable range of measurement is from 1 to 6,000,000 mPa·s. A hybrid nanolubricant sample of 16 mL was poured into a cylindrical container and attached to the rheometer. The dynamic viscosity of the testing sample was measured by several spindle rotational speeds and data was collected by a RheoCal program. The measurement sample of dynamic viscosity was conducted for a temperature range from 30 to 80 °C. The temperature of a testing sample was controlled by a circulating water bath. The measurement was repeated three times and the average value was considered. The apparatus setup was validated using a 40:60 EG base liquid mixture at different temperatures and compared with existing data in the literature [39]. Moreover, the measurements of thermal conductivity and dynamic viscosity were conducted for G-Al<sub>2</sub>O<sub>3</sub> hybrid nanolubricants.

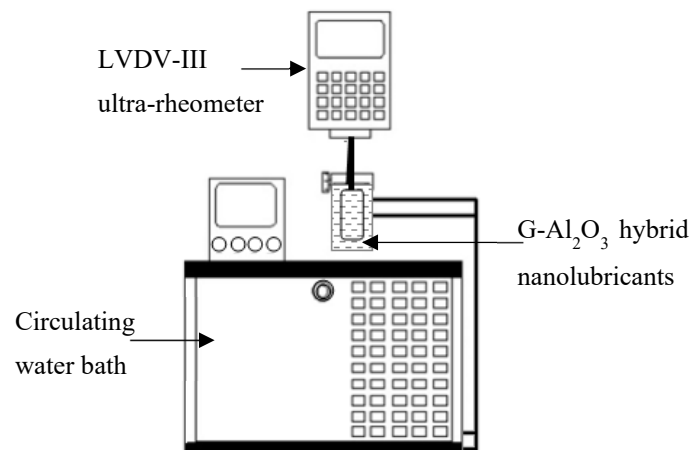


**Figure 5.** Schematic of the dynamic viscosity measurement.

#### 2.5. Tribological Characteristics Measurement

The measurements of tribological properties of all G-Al<sub>2</sub>O<sub>3</sub> hybrid nanolubricants samples were performed using a four-ball wear tribotester (Ducom TR-30 L) machine by following the ASTM D4172 standard. The variation of friction coefficient at the rubbing interface of four chrome steel balls in AISI 52100 standard with a diameter of 12.7 mm, a hardness value of 62 HRC, and extra polished of grade 25, was evaluated. Figure 6 shows the schematic experiment of a steel ball that was fastened on a collector, while the other three stationary balls were clamped together in the pot and then covered with approximately 10 mL of hybrid nanolubricant sample for each test. The experimental

procedures followed the ASTM D4172 standard by conducting the experiment for one hour while maintaining a rotation velocity of 1200 r/min, and under a load of 392 N at a constant temperature of 75 °C [40]. The four-ball tribology test was conducted by rubbing process to evaluate the friction coefficient of the hybrid nanolubricants sample. Equation (3) was implemented by Windcom Data software through a specific data acquisition system from the four-ball wear tribotester, and the results of the friction coefficient were analyzed and displayed on a desktop. In Equation (3), the dimensionless friction coefficient is  $\mu_f$ , and the radial distance between the rotation axis to the center of the contact surface on the lower balls,  $r$  is 3.67 mm.

$$\mu_f = \frac{T_f \cdot \sqrt{6}}{3 \cdot W \cdot r} \quad (3)$$

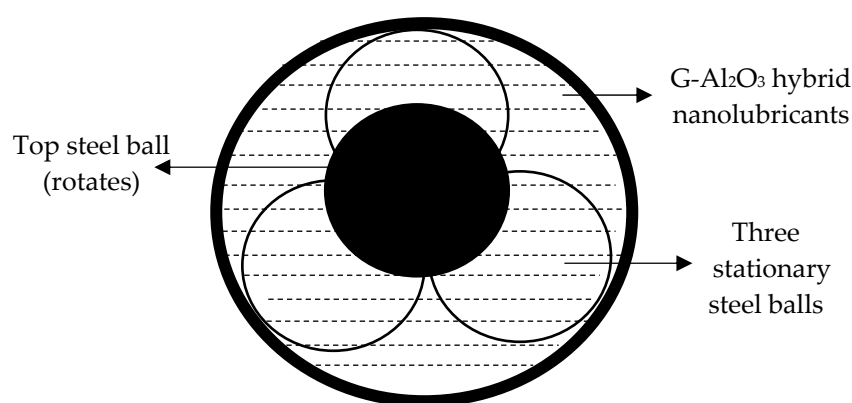


**Figure 6.** Schematic of the steel balls assembly for the four-ball wear test measurement.

### 3. Results and Discussion

#### 3.1. Stability of G-Al<sub>2</sub>O<sub>3</sub> Hybrid Nanolubricants

The stability of the G-Al<sub>2</sub>O<sub>3</sub> hybrid nanolubricant was further determined by the absorbance ratio,  $\bar{A}_r$  as presented in Figure 7. The  $\bar{A}_r$  indicates the ratio of final absorbance,  $\bar{A}$  refers to a specific sedimentation time towards the initial absorbance, and  $\bar{A}_0$  refers to that of the reference fluid (base liquid mixture). In the sedimentation period, the ideal absorbance ratio is obtained when  $\bar{A}_r$  is closer to 1 or 100%, which shows an excellent stability of hybrid nanolubricants sample. Few researchers [41,42] have used UV-Vis spectrometry to carry out experimental investigation on engineering-fluid stability. Absorbance ratios of G-Al<sub>2</sub>O<sub>3</sub> hybrid nanolubricants for different ultra-sonication and sedimentation time periods were measured regularly over 336 h for a specific wavelength of 550 nm. A time period of 2 h ultra-sonication achieved stable samples for four samples in various ultra-sonication time periods from 0 to 3 h. Samples attained an absorbance ratio of more than 70% for up to two weeks of sedimentation period. However, the poor stability condition for samples without ultra-sonication and for a 0.5 h ultra-sonication time were determined to be unstable as the absorbance ratio was smaller than 25% and 40% after two weeks, respectively. Here, the condition of samples started to deteriorate with sedimentation time. Sharif et al. [41] and Habibzadeh et al. [43] also suggested a typical method of measurements for optimum stability conditions. Therefore, the UV-Vis spectrophotometer is capable of determining the stability of the dispersion of suspended hybrid nanoparticles in lubricant samples. The preparation of samples with 2 h ultra-sonication time periods was executed for measurements of thermal conductivity, dynamic viscosity, and tribological characterization of G-Al<sub>2</sub>O<sub>3</sub> hybrid nanolubricants in several hybrid ratios.



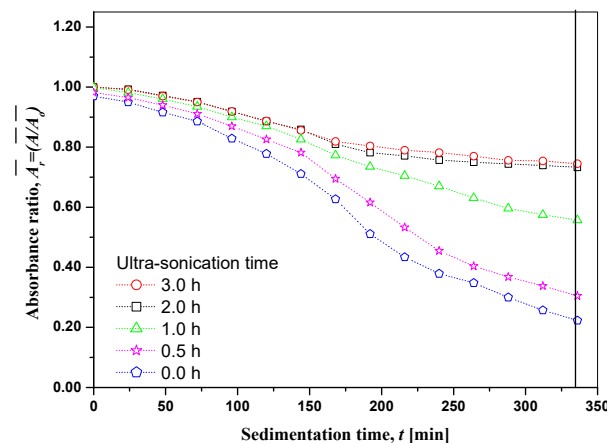


**Figure 7.** Absorbance ratio for different ultra-sonication time periods.

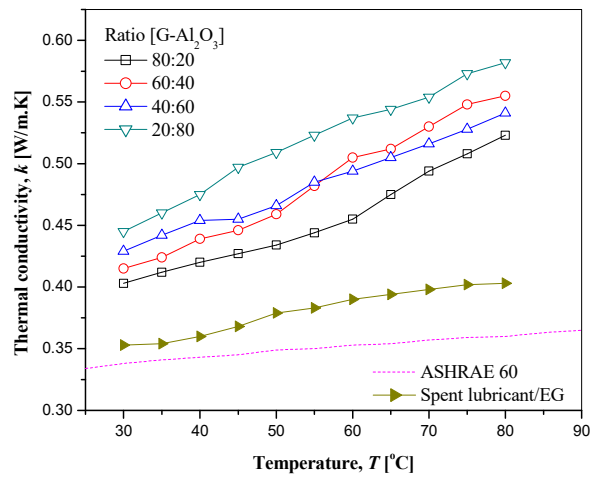
### 3.2. Thermal Conductivity of G-Al<sub>2</sub>O<sub>3</sub> Hybrid Nanolubricants

The thermal conductivity was validated with a correlation process of the present results as compared to ASHRAE [44] for a 60% ethylene glycol (40:60) aqueous mixture. The validation results for the thermal conductivity measurements were obtained in a similar increasing pattern in the same temperature ranges using the KD2 Pro Thermal Analyzer, as depicted in Figure 8a.

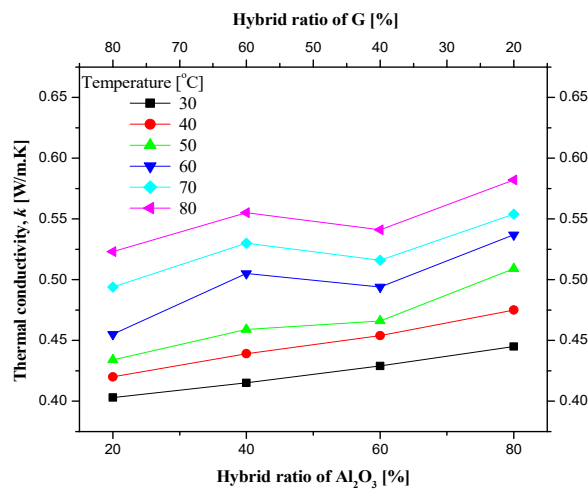
Figure 8a shows the thermal conductivity for 1.0% volume concentration of various G-Al<sub>2</sub>O<sub>3</sub> nanoparticle hybrid ratios at several temperatures. The thermal conductivity of all hybrid ratios G-Al<sub>2</sub>O<sub>3</sub> nanolubricants significantly increased with temperature as compared with their base liquid mixture. The hybrid ratio of 20:80 G-Al<sub>2</sub>O<sub>3</sub> nanolubricants obtained the highest thermal conductivity in all temperature ranges. Nevertheless, the ratio of 60:40 (G-Al<sub>2</sub>O<sub>3</sub>) provided slightly better thermal conductivity as compared to the 40:60 (G-Al<sub>2</sub>O<sub>3</sub>) lubricant sample due to the possibility of nanoparticles agglomeration since within the cluster, heat could transfer rapidly in volume fraction of conductive phase in order to increase thermal conductivity [45]. Meanwhile, the thermal conductivity of the ratio 80:20 hybrid nanolubricant was found to be the lowest among the hybrid ratios and temperatures researched. The results showed that better thermal conductivity of the G-Al<sub>2</sub>O<sub>3</sub> hybrid nanolubricant was contributed to by higher percentages of Al<sub>2</sub>O<sub>3</sub> nanoparticles, as shown in Figure 8b. According to the present work, hybrid ratios of nanoparticles lead to thermal conduction improvement due to two nanoparticles of different sizes and the quantity of the smaller nanoparticles suspend in the mixture. The diameter size of Al<sub>2</sub>O<sub>3</sub> nanoparticles is approximately 13 nm and it is smaller than the graphene nanoparticles; thus, the Al<sub>2</sub>O<sub>3</sub> nanoparticles play a significant role in thermal conduction by occupying the empty space between the bigger graphene nanoparticles, as observed from the TEM image in Figure 2b. The random and excellent suspension of the two nanoparticles in the hybrid liquid sample mixtures enhances the thermal conductivity by the increment of contact area among the molecules. Hence, it induced greater heat transfer rates throughout the collision of nanoparticles through Brownian motion [46].

The effective thermal conductivity of G-Al<sub>2</sub>O<sub>3</sub> hybrid nanolubricants and its related augmentation is presented in Figure 8c. The results show that the effective thermal conductivity increases as the Al<sub>2</sub>O<sub>3</sub> nanoparticles ratio in nanolubricant samples is increased, except for the ratio of 60:40 where it is slightly better than the ratio of 40:60 (G-Al<sub>2</sub>O<sub>3</sub>) at temperatures higher than 50 °C. The effective thermal conductivity of the G-Al<sub>2</sub>O<sub>3</sub> hybrid nanolubricant was inversely proportional to the concentration ratio of graphene particles for each set of temperatures, except the ratio of 60:40 (G-Al<sub>2</sub>O<sub>3</sub>) after 50 °C. Temperature significantly contributes to the effective thermal conductivity percentages. Furthermore, at an operating temperature of 80 °C, the maximum enhancement was evaluated to be enhanced by approximately 29% for a hybrid ratio of 20:80 (G-Al<sub>2</sub>O<sub>3</sub>) nanolubricants. This is probably

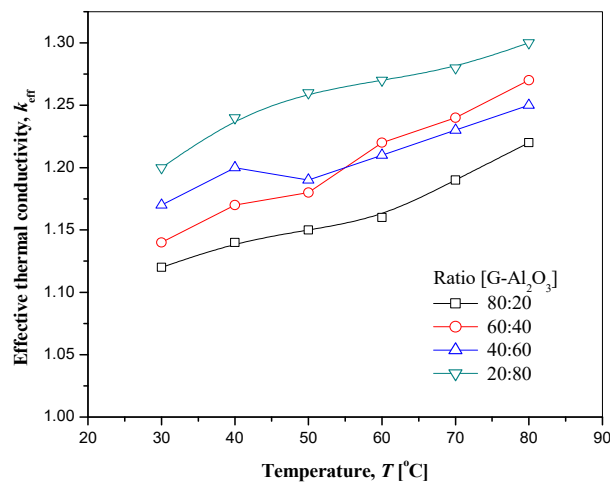
due to more kinetic energy being converted at high temperatures to increase the interaction of nanoparticles between each other in the free Brownian motion solution [46,47].



(a)



(b)

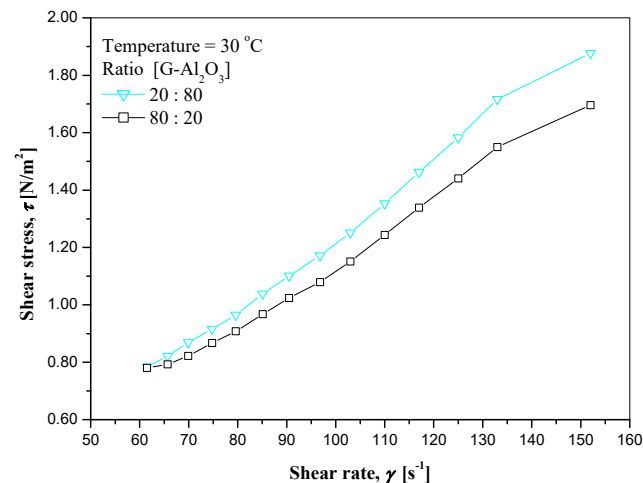


(c)

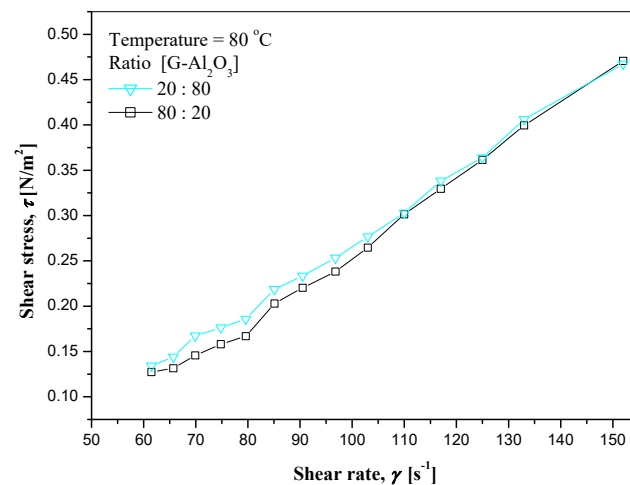
**Figure 8.** Experimental thermal conductivity of G- $\text{Al}_2\text{O}_3$  hybrid nanolubricants. (a) Variation of thermal conductivity with temperatures; (b) variation of thermal conductivity with hybrid ratios; (c) thermal conductivity enhancement of G- $\text{Al}_2\text{O}_3$  hybrid nanolubricants.

### 3.3. Dynamic Viscosity of G-Al<sub>2</sub>O<sub>3</sub> Hybrid Nanolubricants

Figure 9 presents the shear stress versus shear rate in the range of  $60 < \dot{\gamma} < 150 \text{ s}^{-1}$  for hybrid ratios of 80:20 and 20:80 of G-Al<sub>2</sub>O<sub>3</sub> nanolubricants at temperatures of 30 °C and 80 °C, respectively. The measured data show that the shear rates against shear stress linearly increase at temperatures of 30 °C and 80 °C in Figure 9a,b, respectively. The data examined showed that the G-Al<sub>2</sub>O<sub>3</sub> hybrid nanolubricants behaved as Newtonian fluids within the temperatures studied. The dynamic viscosity of hybrid 80:20 G-Al<sub>2</sub>O<sub>3</sub> nanolubricants is lower than the ratio of 20:80 for both temperatures, as presented in Figure 9a,b. This can be due to variation in the amounts of nanoparticles of graphene and Al<sub>2</sub>O<sub>3</sub> in hybrid ratios of 80:20 and 20:80 (G-Al<sub>2</sub>O<sub>3</sub>). A similar finding was also observed by Hamid et al. [48] for SiO<sub>2</sub>-TiO<sub>2</sub> nanofluids. They found that the SiO<sub>2</sub>-TiO<sub>2</sub> nanofluids obtained Newtonian fluid behavior for the ratio of 50:50 at temperatures of 50 °C and 30 °C. Dynamic viscosity was validated by comparing the collected results with ASHRAE [45] for the 60% ethylene glycol mixture. The validation viscosity results were in acceptable trend with ASHRAE data for a similar range of temperatures, as illustrated in Figure 10a. Based on the evaluated results, the base liquid of the spent lubricant/EG (40:60) mixture fits closely with the ASHRAE trend of pattern, and the dynamic viscosity decreased exponentially with the temperatures.



(a)

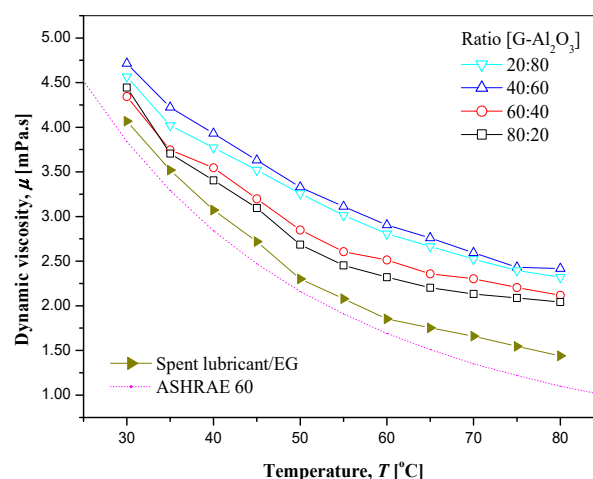


(b)

**Figure 9.** Shear stress versus shear rate for various G-Al<sub>2</sub>O<sub>3</sub> hybrid nanolubricants. (a) Shear stress against shear rate at temperature of 30 °C; (b) shear stress against shear rate at temperature of 80 °C.

Figure 10a demonstrates the dynamic viscosity of nanolubricants of several G-Al<sub>2</sub>O<sub>3</sub> hybrid ratios for nanoparticles having a volume concentration of 1.0% within a temperature range from 30 to 80 °C. The dynamic viscosity exponentially decreased with temperatures for all hybrid ratios, which followed the pattern of the base liquid mixture trend. This is probably due to the temperature increments weakening intermolecular interactions between the molecules, thus decreasing the dynamic viscosity value [49]. The dynamic viscosity of hybrid ratios of 80:20, 60:40 and 20:80 (G-Al<sub>2</sub>O<sub>3</sub>) was lower as compared to the value of the 40:60 ratio for all temperatures. Figure 10b presents the dynamic viscosity variation with the percentages of hybrid ratios for graphene and Al<sub>2</sub>O<sub>3</sub> nanoparticle intensities in some mixture lubricants. The nanoparticles hybrid ratio of 40:60 produced the highest data of dynamic viscosity from 30 to 80 °C. The dynamic viscosity of the testing sample slightly decreased with the lower content of Al<sub>2</sub>O<sub>3</sub> nanoparticles. The discrepancy in hybrid ratio of graphene and Al<sub>2</sub>O<sub>3</sub> nanoparticles in the lubricant mixture contributed to the various interactions of those nanoparticles with base liquid mixture [50]. Furthermore, the effects of temperature on the dynamic viscosity for all hybrid ratios of G-Al<sub>2</sub>O<sub>3</sub> nanolubricants are reduced by the increasing temperature; this was confirmed by other researchers [50,51].

The variation of relative dynamic viscosity of G-Al<sub>2</sub>O<sub>3</sub> hybrid nanolubricants with temperature is depicted in Figure 10c. According to the figure, all hybrid ratio samples attained the maximum value in relative dynamic viscosity at a temperature of 80 °C. The dynamic viscosity relative ratio of 40:60 (G-Al<sub>2</sub>O<sub>3</sub>) increased from 30 to 50 °C, then the ratio remained constant at temperatures of 60–80 °C. Furthermore, the ratios of 20:80 and 80:20 also attained a similar pattern in relative dynamic viscosity with approximately 22% enhancement for temperatures up to 50 °C, and the results were significantly improved for a temperature range of 60–80 °C. The maximum increment of 40:60 hybrid ratio is approximately 40% as compared to the base liquid mixture at temperature of 80 °C. Nevertheless, the relative dynamic viscosity smoothly increased with the increasing of temperature for the hybrid ratio of 60:40 (G-Al<sub>2</sub>O<sub>3</sub>). This revealed that the relative dynamic viscosity distribution for all hybrid ratio samples was below the 40:60 ratio throughout the studied range of temperatures. The fluctuation data did not show any specific trend at different hybrid ratios. This behavior is related to several shearing flow resistance effects due to two types of nanoparticles that have different particles sizes and structures in various hybrid ratios [39].



(a)

Figure 10. Cont.

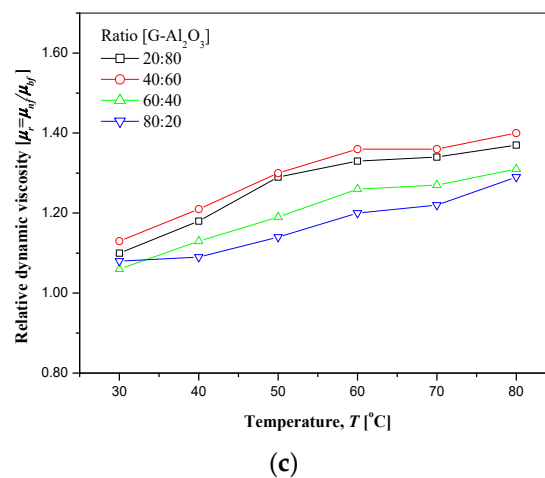
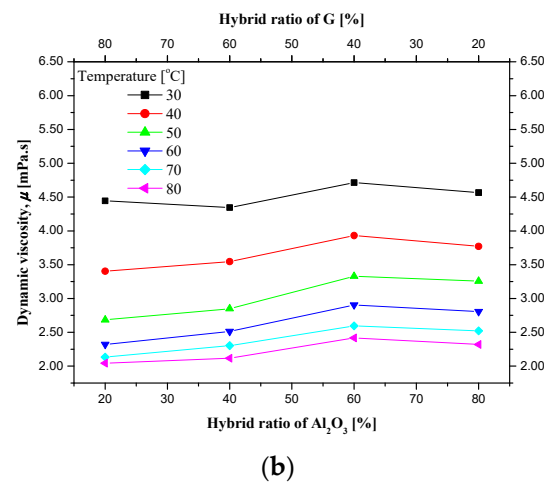


**Figure 10.** Experimental dynamic viscosity of G-Al<sub>2</sub>O<sub>3</sub> hybrid nanolubricants. (a) Variation of dynamic viscosity with temperature; (b) variation of dynamic viscosity with hybrid ratios; (c) variation of relative dynamic viscosity for different hybrid ratios.

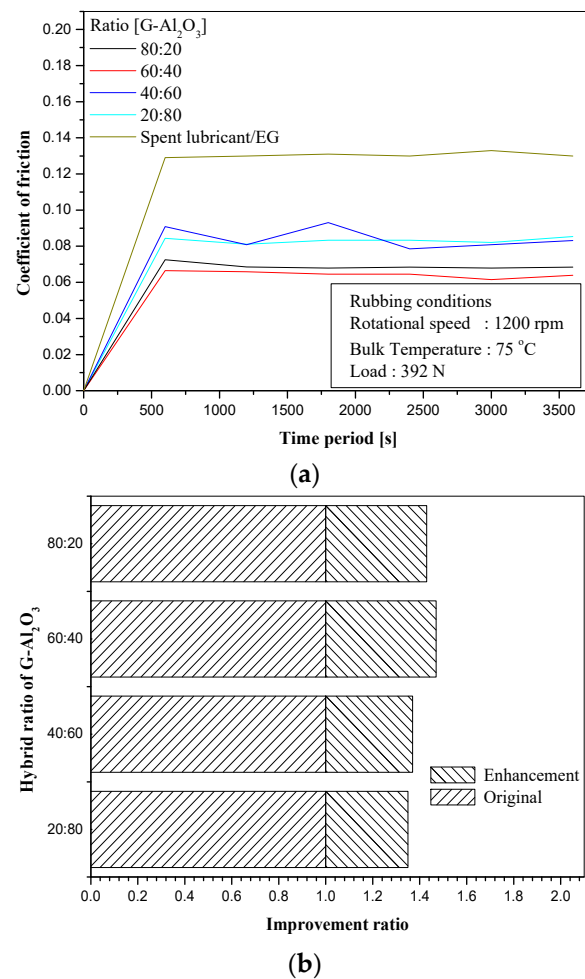
### 3.4. Friction Coefficient (COF) Assessment for G-Al<sub>2</sub>O<sub>3</sub> Hybrid Nanolubricants

Figure 11 presents the distribution of friction coefficient with the rubbing time for all nanolubricant samples of different hybrid ratios in 1.0% nanoparticle volume concentration. The lubrication effect occurred during the four-ball wear test within the boundary lubrication state [52,53]. The general behavior of fluid cooling lubrication is shown as a function of velocity, viscosity, contact area and load, according to the Stribeck curve [40]. As the viscosity was inversely proportional to the lubricants' temperature, film thickness might decrease and cause a shift along the Stribeck curve into the boundary lubrication effect. The presence of nanoparticles at different concentrations interacts with the steel surface structures [54].

Figure 11a shows the results of tribological experimentation for different G-Al<sub>2</sub>O<sub>3</sub> hybrid nanolubricant samples with hybrid ratios of 20:80, 40:60, 60:40 and 80:20 in a 1.0% volume concentration condition. The ratio of 60:40 (G-Al<sub>2</sub>O<sub>3</sub>) obtained the lowest friction coefficient values among all the hybrid ratios in time periods of 3600 s of experiment. The maximum enhancement of the friction coefficient value was evaluated at a hybrid ratio of 60:40 of G-Al<sub>2</sub>O<sub>3</sub> hybrid nanolubricants with a 45% reduction as compared to the base liquid mixture, as presented in Figure 11b. The collected data showed that the greater percentage of graphene particles contribute to the smaller value in friction coefficient of the G-Al<sub>2</sub>O<sub>3</sub> hybrid nanolubricants. This is because adhesion of graphene on an atomically smooth surface and the ease of shear on its tight packed structure provided excellent tribological properties with a significant reduction in friction [30]. Mungse and Khatri [55]



proved that the film formed by graphene nanoparticles on the friction surface reduced the friction coefficient by approximately 14%.

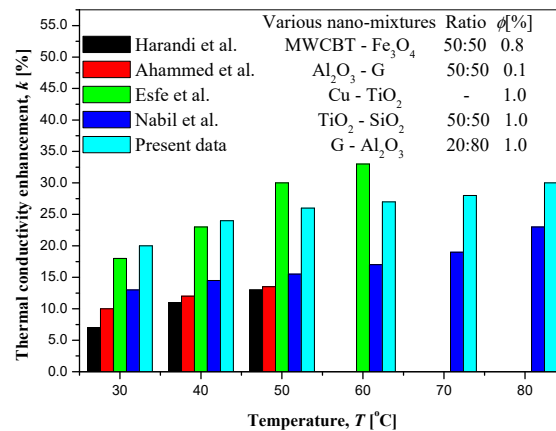


**Figure 11.** Variation of friction coefficient of G-Al<sub>2</sub>O<sub>3</sub> hybrid nanolubricants. (a) Friction for nanolubricants of various hybrid ratios after the four-ball tribotest; (b) friction enhancement of G-Al<sub>2</sub>O<sub>3</sub> hybrid nanolubricants.

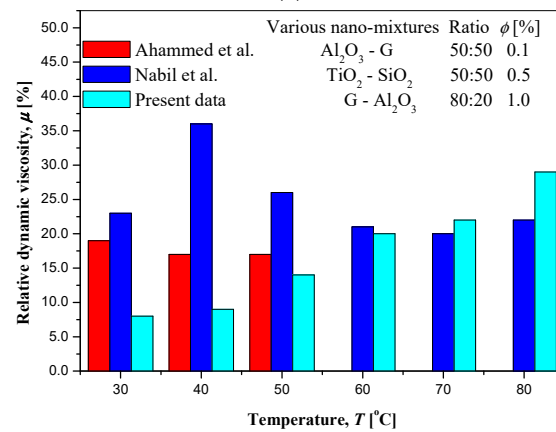
### 3.5. Comparison with the Literature

Figure 12a presents the effective thermal conductivity correlation study between present data with the results from Esfe et al. [20], Nabil et al. [39], Harandi et al. [50], and Ahammed et al. [56]. The present study achieved an enhancement in thermal conductivity of G-Al<sub>2</sub>O<sub>3</sub> hybrid nanolubricants by 20–30% compared to the base mixture. Nabil et al. [39] demonstrated an investigation of thermal conductivity for SiO<sub>2</sub>-TiO<sub>2</sub> nanomixtures with 50:50 ratio in a water-EG base liquid mixture. They measured enhancements in thermal conductivity of 10–25% higher than the base liquid mixture, which is approximately 7% less than the present study at 80 °C and 1.0% nanoparticle volume concentration. Ahammed et al. [56] used water-based Al<sub>2</sub>O<sub>3</sub>-graphene nanoparticles as nanomixtures. They reported that the effective thermal conductivity of nanomixtures with 0.1% nanoparticle concentration was at least 15% higher than the water base liquid mixture at a temperature of 50 °C. Furthermore, Esfe et al. [20] used Cu-TiO<sub>2</sub> nanomixtures for 1.0% nanoparticle concentration at an unknown ratio through a water-EG mixture as the base liquid solution. Their enhancement of thermal conductivity was approximately 15% higher than that of the present study at temperature 60 °C. Harandi et al. [50] determined that the thermal conductivity augmentation percentage for nanomixtures of

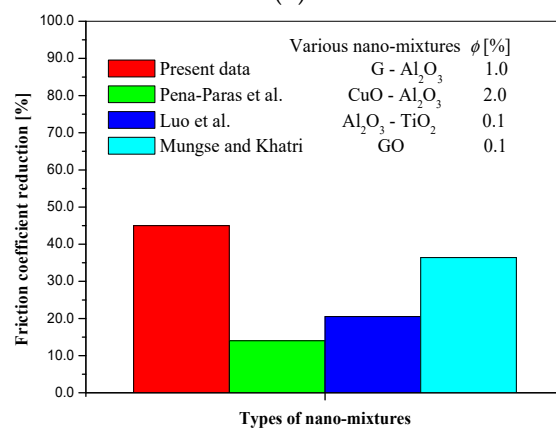
$\text{Al}_2\text{O}_3\text{-G}$  was higher than that of the  $\text{MWCBT-Fe}_3\text{O}_4$ , even at lower nanoparticle volume concentrations of 0.8%.



(a)



(b)



(c)

**Figure 12.**  $\text{G-Al}_2\text{O}_3$  hybrid nanolubricants compared with the literature in terms of friction and thermo-physical properties. (a) Thermal conductivity comparison; (b) dynamic viscosity comparison; (c) comparison of friction improvement.

Figure 12b exhibits the relative dynamic viscosity of the collected present results with 1.0% volume concentration as compared to others at 0.1% and 0.5% concentrations. Ahammed et al. [56] conducted a study of dynamic viscosity for  $\text{Al}_2\text{O}_3$ -graphene nanoparticles suspended in a water base. The relative dynamic viscosity in their experiments were higher than the present data for temperatures of 30–50 °C, and more than double as compared to the present data at temperatures of 30 °C and 40 °C. Nabil et al. [39]

demonstrated dynamic viscosity measurements of 50:50 ratio  $\text{TiO}_2\text{-SiO}_2$  nanomixtures for a 0.5% nanoparticle concentration. They obtained the highest relative ratio of 1.35 at a temperature of 40 °C. The present data showed lower relative dynamic viscosity ratios for temperatures between 30 and 60 °C, which were then 1.22 and 1.29 at temperatures of 50 °C and 60 °C, respectively, as compared to this paper. Sundar et al. [57] reported that the magnitude of relative dynamic viscosity or thermal conductivity enhancement depends on the types of nanoparticles and base liquid mixtures. These were observed and are illustrated in Figure 12a,b.

The coefficient of friction reduction by the present data with a 1.0% volume concentration of 60:40 hybrid ratio (G- $\text{Al}_2\text{O}_3$ ) attained the highest percentage of 45% as compared to others as presented in Figure 12c. Luo et al. [27] used  $\text{Al}_2\text{O}_3\text{-TiO}_2$  hybrid nanomixtures with 0.1% concentration for friction test measurement. Their results showed a 16% lower coefficient of friction than that obtained by Mungse and Khatir [55], who used GO nanomixtures with a 0.1% concentration, but 6% higher as compared to the results obtained by Pena-Paras et al. [58], who used  $\text{CuO-Al}_2\text{O}_3$  nanoparticles with a 2.0% concentration. Furthermore, the present data resulted in better anti-friction characteristic with 30%, 14% and 8% as compared to  $\text{CuO-Al}_2\text{O}_3$  (2.0% concentration) nanoparticles,  $\text{Al}_2\text{O}_3\text{-TiO}_2$  (0.1% concentration) nanoparticles and GO (0.1% concentration) nanoparticles, respectively. According to Ali et al. [26], the friction of graphene on rubbing surfaces depends on the strength of the graphene adhesion to the atomically smooth or rough surface.

### 3.6. Properties Enhancement Ratio

G- $\text{Al}_2\text{O}_3$  hybrid nanolubricants with a good combination assessment for dynamic viscosity and thermal conductivity could be determined by the properties enhancement ratio. This was calculated using Equation (4), which is the increased ratio of relative dynamic viscosity divided by the relative thermal conductivity of base liquid mixtures [48,59].

$$PER = (\mu_r - 1) / (k_{eff} - 1) \quad (4)$$

According to Garg et al. [59], the dimensionless values of  $PER$  are located in the area below 5 for good heat transfer, while the area above 5 did not help heat transfer. Figure 13 illustrates the  $PER$  for the G- $\text{Al}_2\text{O}_3$  hybrid nanolubricants in the temperature range from 30 to 80 °C. The hybrid ratios of 20:80 and 60:40 fall below the line of area 5 value  $PER$ , but few points were above the line for temperatures of 70–80 °C. Meanwhile, the  $PER$  was higher than the value 5 for 40:60 and 80:20 ratios, were not good heat transfer liquids and are not suggested for cooling lubrication application. Therefore, the minimum quantity cooling lubrication (MQCL) system will be enhanced using the advantages of G- $\text{Al}_2\text{O}_3$  hybrid nanolubricants with ratios of 60:40 and 20:80 in cooling the temperature of mechanical parts.

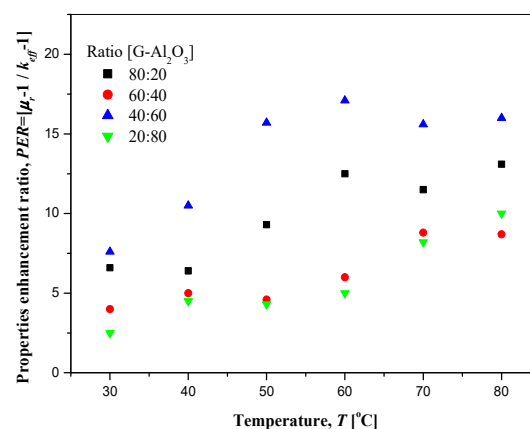


Figure 13. Properties enhancement ratio against temperature for several hybrid ratios.

#### 4. Conclusions

The thermo-physical properties, such as thermal conductivity and dynamic viscosity, and tribological characteristics of 1.0% G-Al<sub>2</sub>O<sub>3</sub> volume concentration hybrid nanolubricants were investigated for four hybrid ratios through temperatures from 30 to 80 °C. Samples prepared by a 2 h ultra-sonication process were observed to obtain maximum stability, whereby the absorbance ratio was above 70% after a two-week sedimentation period. The highest percentage of relative dynamic viscosity was obtained by the 40:60 hybrid ratio with a 30% increment. Meanwhile, the average effective thermal conductivity enhancement of the sample was approximately 1.25 times for hybrid ratio 20:80 (G-Al<sub>2</sub>O<sub>3</sub>) in the ranges of temperatures measured. By comparing with other ratios, the hybrid ratio 60:40 provided the maximum improvement of up to 45% in the coefficient of friction reduction. In terms of the properties enhancement ratio, it is estimated that the hybrid ratios of 20:80 and 60:40 had given adequate aid in heat dissipation through the combination of thermal conductivity augmentation and relative dynamic viscosity as compared to other hybrid ratios. Further experiments and investigations on the performance of introducing G-Al<sub>2</sub>O<sub>3</sub> hybrid nanolubricants into the MQL system in machining application are required to extend the present study.

**Author Contributions:** Conceptualization, W.H.A. and A.R.Y.; methodology, W.H.A.; software, S.K.L.; validation, W.H.A., S.K.L. and A.R.Y.; formal analysis, S.K.L.; investigation, S.K.L.; resources, A.R.Y.; data curation, A.S.J.; writing—original draft preparation, S.K.L.; writing—review and editing, A.R.Y.; visualization, A.S.J.; supervision, A.R.Y.; project administration, A.R.Y.; funding acquisition, A.S.J. All authors have read and agreed to the published version of the manuscript.

**Funding:** University Malaysia Pahang (UMP) grant RDU 210365 and Malaysia Ministry of Higher Education FRGS/1/2022/TK10/UMP/02/57.

**Data Availability Statement:** Data sharing not applicable.

**Acknowledgments:** The authors are grateful to the Malaysia Ministry of Higher Education and University Malaysia Pahang (UMP) for financial support. This work was supported by the UMP grant RDU 210365 and FRGS/1/2022/TK10/UMP/02/57.

**Conflicts of Interest:** The authors declare no conflict of interest.

#### References

1. Pereira, O.; Martin-Alfonso, J.E.; Rodriguez, A.; Calleja, A.; Fernandez-Valdivielso, A.; Lopez de Lacalle, L.N. Sustainability analysis of lubricant oils for minimum quantity lubrication based on their tribo-rheological performance. *J. Clean. Prod.* **2017**, *164*, 1419–1429. [[CrossRef](#)]
2. Debnath, S.; Reddy, M.M.; Qua, S.Y. Environmental friendly cutting fluids and cooling techniques in machining: A review. *J. Clean. Prod.* **2014**, *83*, 33–47. [[CrossRef](#)]
3. Amiril, S.A.S.; Rahim, E.A.; Sharif, S.; Sasahara, H. Machining performance of vegetable oil with phosphonium- and ammonium-based ionic liquids via MQL technique. *J. Clean. Prod.* **2019**, *209*, 947–964.
4. Kumar, N.; Sonawane, S.S. Experimental study of Fe<sub>2</sub>O<sub>3</sub>/water and Fe<sub>2</sub>O<sub>3</sub>/ethylene glycol nanofluids heat transfer enhancement in a shell and tube heat exchanger. *Int. Commun. Heat Mass Transf.* **2016**, *78*, 277–284. [[CrossRef](#)]
5. Naghash, A.; Sattari, S.; Rashidi, A. Experimental assessment of convective heat transfer coefficient enhancement of nanofluids prepared from high surface area nanoporous graphene. *Int. Commun. Heat Mass Transf.* **2016**, *78*, 127–134. [[CrossRef](#)]
6. Agarwal, D.K.; Vaidyanathan, A.; Sunil Kumar, S. Investigation on convective heat transfer behaviour of kerosene-Al<sub>2</sub>O<sub>3</sub> nanofluid. *Appl. Therm. Eng.* **2015**, *84*, 64–73. [[CrossRef](#)]
7. Saleh, R.; Putra, N.; Wibowo, R.E.; Septiadi, W.N.; Prakoso, S.P. Titanium dioxide nanofluids for heat transfer applications. *Exp. Therm. Fluid Sci.* **2014**, *52*, 19–29. [[CrossRef](#)]
8. Lim, S.K.; Azmi, W.H.; Yusoff, A.R. Investigation of thermal conductivity and viscosity of Al<sub>2</sub>O<sub>3</sub>/water-ethylene glycol mixture nanocoolant for cooling channel of hot-press forming die application. *Int. Commun. Heat Mass Transf.* **2016**, *78*, 182–189. [[CrossRef](#)]
9. Said, Z.; Sabiha, M.A.; Saidur, R.; Hepbasli, A.; Rahim, N.A.; Mekhilef, S.; Ward, T.A. Performance enhancement of a flat plate solar collector using titanium dioxide nanofluid and polyethylene glycol dispersant. *J. Clean. Prod.* **2015**, *92*, 343–353. [[CrossRef](#)]
10. Peyghambarzadeh, S.M.; Hashemabadi, S.H.; Hoseini, S.M.; Seifi Jamnani, M. Experimental study of heat transfer enhancement using water/ethylene glycol based nanofluids as a new coolant for car radiators. *Int. Commun. Heat Mass Transf.* **2011**, *38*, 1283–1290. [[CrossRef](#)]

11. Botha, S.S.; Ndungu, P.; Bladergroen, B.J. Physicochemical properties of oil-based nanofluids containing hybrid structures of silver nanoparticles supported on silica. *Ind. Eng. Chem. Res.* **2011**, *50*, 3071–3077. [[CrossRef](#)]
12. Minea, A.A. Hybrid nanofluids based on Al<sub>2</sub>O<sub>3</sub>, TiO<sub>2</sub> and SiO<sub>2</sub>: Numerical evaluation of different approaches. *Int. J. Heat Mass Transf.* **2017**, *104*, 852–860. [[CrossRef](#)]
13. Yarmand, H.; Gharekhani, S.; Shirazi, S.F.S.; Goodarzi, M.; Amiri, A.; Sarsam, W.S.; Alehashem, M.S.; Dahari, M.; Kazi, S.N. Study of synthesis, stability and thermophysical properties of graphene nanoplatelet/platinum hybrid nanofluid. *Int. Commun. Heat Mass Transf.* **2016**, *77*, 15–21. [[CrossRef](#)]
14. Bahrami, M.; Akbari, M.; Karimipour, A.; Afrand, M. An experimental study on rheological behaviour of hybrid nanofluids made of iron and copper oxide in a binary mixture of water and ethylene glycol: Non-Newtonian behaviour. *Exp. Therm. Fluid Sci.* **2016**, *79*, 231–237. [[CrossRef](#)]
15. Madhesh, D.; Parameshwaran, R.; Kalaiselvam, S. Experimental investigation on convective heat transfer and rheological characteristics of Cu-TiO<sub>2</sub> hybrid nanofluids. *Exp. Therm. Fluid Sci.* **2014**, *52*, 104–115. [[CrossRef](#)]
16. Sundar, L.S.; Singh, M.K.; Sousa, A.C.M. Enhanced heat transfer and friction factor of MWCNT-Fe<sub>3</sub>O<sub>4</sub>/water hybrid nanofluids. *Int. Commun. Heat Mass Transf.* **2014**, *52*, 73–83. [[CrossRef](#)]
17. Akilu, S.; Sharma, K.V.; Baheta, A.T.; Mamat, R. A review of thermophysical properties of water based composite nanofluids. *Renew. Sustain. Energy Rev.* **2016**, *66*, 654–678. [[CrossRef](#)]
18. Lim, S.K.; Mohamad, N.Z.; Yusoff, A.R. Experimental investigation of recycled machining coolant mixed with nanofluids based Al<sub>2</sub>O<sub>3</sub>. *IOP Conf. Ser. Mater. Sci. Eng.* **2019**, *530*, 012002. [[CrossRef](#)]
19. Ho, C.J.; Huang, J.B.; Tsai, P.S.; Yang, Y.M. Preparation and properties of hybrid water-based suspension of Al<sub>2</sub>O<sub>3</sub> nanoparticles and MEPCM particles as functional forced convection fluid. *Int. Commun. Heat Mass Transf.* **2010**, *37*, 490–494. [[CrossRef](#)]
20. Esfe, M.H.; Arani, A.A.A.; Rezaie, M.; Yan, W.M.; Karimipour, A. Experimental determination of thermal conductivity and dynamic viscosity of Ag-MgO/water hybrid nanofluid. *Int. Commun. Heat Mass Transf.* **2015**, *66*, 189–195. [[CrossRef](#)]
21. Soltani, O.; Akbari, M. Effects of temperature and particles concentration on the dynamic viscosity of MgO-MWCNT/ethylene glycol hybrid nanofluids: Experimental study. *Physica E* **2016**, *84*, 564–570. [[CrossRef](#)]
22. Baghbanzadeh, M.; Rashidi, A.; Rashtchian, D.; Lotfi, R.; Amrollahi, A. Synthesis of spherical silica/multiwall carbon nanotubes hybrid nanostructures and investigation of thermal conductivity of related nanofluids. *Thermochim. Acta* **2012**, *549*, 87–94. [[CrossRef](#)]
23. Jana, S.; Salehi-Khojin, A.; Zhong, W.H. Enhancement of fluid thermal conductivity by the addition of single and hybrid nano-additives. *Thermochim. Acta* **2007**, *462*, 45–55. [[CrossRef](#)]
24. Suresh, S.; Venkitaraj, K.P.; Selvakumar, P.; Chandrasekar, M. Synthesis of Al<sub>2</sub>O<sub>3</sub>-Cu/water hybrid nanofluids using two step method and its thermo physical properties. *Colloids Surf. A* **2011**, *388*, 41–48. [[CrossRef](#)]
25. Kumar, M.S.; Vasu, V.; Gopal, A.V. Thermal conductivity and rheological studies for Cu-Zn hybrid nanofluids with various base fluids. *J. Taiwan Inst. Chem. Eng.* **2016**, *66*, 321–327. [[CrossRef](#)]
26. Ali, I.; Basheer, A.A.; Kucherova, A.; Memetov, N.; Pasko, T.; Ovchinnikov, K.; Pershin, V.; Kuznetsov, D.; Galunin, E.; Grachev, V.; et al. Advances in carbon nanomaterials as lubricants modifiers. *J. Mol. Liq.* **2019**, *279*, 251–266. [[CrossRef](#)]
27. Luo, T.; Wei, X.W.; Zhao, H.Y.; Cai, G.Y.; Zheng, X.Y. Tribology properties of Al<sub>2</sub>O<sub>3</sub>/TiO<sub>2</sub> nanocomposites as lubricant additives. *Ceram. Int.* **2014**, *40*, 10103–10109. [[CrossRef](#)]
28. Alimirzaloo, V.; Qaleh, S.S.G.; Keshtiban, P.M.; Ahmadi, S. Investigation of the effect of CuO and Al<sub>2</sub>O<sub>3</sub> nanolubricants on the surface roughness in the forging process of aluminium alloy. *J. Eng. Tribol.* **2017**, *231*, 1595–1604.
29. Cheng, Z.L.; Qin, X.X. Study on friction performance of graphene-based semi-solid grease. *Chin. Chem. Lett.* **2014**, *25*, 1305–1307. [[CrossRef](#)]
30. Kumar, P.; Wani, M.F. Tribological characterization of graphene oxide as lubricant additive on hypereutectic Al-25Si/steel tribopair. *Tribol. Trans.* **2017**, *61*, 335–346. [[CrossRef](#)]
31. Hamid, K.A.; Azmi, W.H.; Mamat, R.; Sharma, K.V. Experimental investigation on heat transfer performance of TiO<sub>2</sub> nanofluids in water-ethylene glycol mixture. *Int. Commun. Heat Mass Transf.* **2016**, *73*, 1046–1058. [[CrossRef](#)]
32. Azmi, W.H.; Sharma, K.V.; Mamat, R.; Najafi, G.; Mohamad, M.S. The enhancement of effective thermal conductivity and effective dynamic viscosity of nanofluids—A review. *Renew. Sustain. Energy Rev.* **2016**, *53*, 1046–1058. [[CrossRef](#)]
33. Zakaria, I.; Azmi, W.H.; Mohamed, W.A.N.W.; Mamat, R.; Najafi, G. Experimental investigation of thermal conductivity and electrical conductivity of Al<sub>2</sub>O<sub>3</sub> nanofluid in water-ethylene glycol mixture for proton exchange membrane fuel cell application. *Int. Commun. Heat Mass Transf.* **2015**, *61*, 61–68. [[CrossRef](#)]
34. Sundar, L.S.; Ramana, E.V.; Singh, M.K.; Sousa, A.C.M. Thermal conductivity and viscosity of stabilized ethylene glycol and water mixture Al<sub>2</sub>O<sub>3</sub> nanofluids for heat transfer applications: An experimental study. *Int. Commun. Heat Mass Transf.* **2014**, *56*, 86–95. [[CrossRef](#)]
35. Abdolbaqi, M.K.; Azmi, W.H.; Mamat, R.; Sharma, K.V.; Najafi, G. Experimental investigation of thermal conductivity and electrical conductivity of bioglycol-water mixture based Al<sub>2</sub>O<sub>3</sub> nanofluid. *Appl. Therm. Eng.* **2016**, *102*, 932–941. [[CrossRef](#)]
36. Yu, W.; Xie, H.Q. A review on nanofluids: Preparation, stability mechanisms, and application. *J. Nanomater.* **2012**, *2012*, 1–17. [[CrossRef](#)]
37. Ghadimi, A.; Saidur, R.; Metselaar, H.S.C. A review of nanofluid stability properties and characterization in stationary conditions. *Int. J. Heat Mass Transf.* **2011**, *54*, 4051–4068.



38. Sundar, L.S.; Ramana, E.V.; Graca, M.P.F.; Singh, M.K.; Sousa, A.C.M. Nanodiamond-Fe<sub>3</sub>O<sub>4</sub> nanofluids: Preparation and measurement of viscosity, electrical and thermal conductivities. *Int. Commun. Heat Mass Transf.* **2016**, *73*, 62–74. [[CrossRef](#)]
39. Nabil, M.F.; Azmi, W.H.; Hamid, K.A.; Mamat, R.; Hagos, F.Y. An experimental study on the thermal conductivity and dynamic viscosity of TiO<sub>2</sub>-SiO<sub>2</sub> nanofluids in water: Ethylene glycol mixture. *Int. Commun. Heat Mass Transf.* **2017**, *86*, 181–189. [[CrossRef](#)]
40. Amiril, S.A.S.; Rahim, E.A.; Embong, Z.; Syahrullail, S. Tribological investigations on the application of oil-miscible ionic liquids additives in modified *Jatropha*-based metalworking fluid. *Tribol. Int.* **2018**, *120*, 520–534. [[CrossRef](#)]
41. Sharif, M.Z.; Azmi, W.H.; Redhwan, A.A.M.; Zawawi, N.N.M. Improvement of nanofluid stability using 4-step UV-Vis spectral absorbency analysis. *J. Mech. Eng.* **2017**, *4*, 233–247.
42. Hajjar, Z.; Rashidi, A.M.; Ghozatloo, A. Enhanced thermal conductivities of graphene oxide nanofluids. *Int. Commun. Heat Mass Transf.* **2014**, *57*, 128–131. [[CrossRef](#)]
43. Habibzadeh, S.; Kazemi-Beydokhti, A.; Khodadadi, A.A.; Mortazavi, Y.; Omanovic, S.; Shariat-Niassar, M. Stability and thermal conductivity of nanofluids of tin dioxide synthesized via microwave-induced combustion route. *Chem. Eng. J.* **2010**, *156*, 471–478. [[CrossRef](#)]
44. ASHRAE. *Handbook Fundamentals*; American Society of Heating, Refrigerating and Air-Conditioning Engineers Inc.: Atlanta, GA, USA, 2006.
45. Shahsavari, A.; Salimpour, M.R.; Saghafiyan, M.; Shafii, M.B. An experiment study on the effect of ultrasonication on thermal conductivity of ferrofluid loaded with carbon nanotubes. *Thermochim. Acta* **2015**, *617*, 102–110. [[CrossRef](#)]
46. Elias, M.M.; Mahbulbul, I.M.; Saidur, R.; Sohel, M.R.; Shahrul, I.M.; Khaleduzzaman, S.S.; Sadeghipour, S. Experimental investigation on the thermo-physical properties of Al<sub>2</sub>O<sub>3</sub> nanoparticles suspended in car radiator coolant. *Int. Commun. Heat Mass Transf.* **2014**, *54*, 48–53. [[CrossRef](#)]
47. Usri, N.A.; Azmi, W.H.; Mamat, R.; Hamid, K.A.; Najafi, G. Thermal conductivity enhancement of Al<sub>2</sub>O<sub>3</sub> nanofluid in ethylene glycol and water mixture. *Energy Procedia* **2015**, *79*, 397–402. [[CrossRef](#)]
48. Hamid, K.A.; Azmi, W.H.; Nabil, M.F.; Mamat, R.; Sharma, K.V. Experimental investigation of thermal conductivity and dynamic viscosity on nanoparticle mixture ratios of TiO<sub>2</sub>-SiO<sub>2</sub> nanofluids. *Int. J. Heat Mass Transf.* **2018**, *116*, 1143–1152. [[CrossRef](#)]
49. Afrand, M.; Toghraie, D.; Ruhani, B. Effects of temperature and nanoparticles concentration on rheological behavior of Fe<sub>3</sub>O<sub>4</sub>-Ag/EG hybrid nanofluid: An experimental study. *Exp. Therm. Fluid Sci.* **2016**, *77*, 38–44. [[CrossRef](#)]
50. Harandi, S.S.; Karimipour, A.; Afrand, M.; Akbari, M.; D'Orazio, A. An experimental study on thermal conductivity of f-MWCNT-Fe<sub>3</sub>O<sub>4</sub>/EG hybrid nanofluid: Effects of temperature and concentration. *Int. Commun. Heat Mass Transf.* **2016**, *76*, 171–177. [[CrossRef](#)]
51. Asadi, M.; Asadi, A. Dynamic viscosity of MWCNT/ZnO-engine oil hybrid nanofluid: An experimental investigation and new correlation in different temperatures and solid concentrations. *Int. Commun. Heat Mass Transf.* **2016**, *76*, 41–45. [[CrossRef](#)]
52. Zulkifli, N.W.M.; Kalam, M.A.; Masjuki, H.H.; Shahabuddin, M.; Yunus, R. Wear prevention characteristics of a palm oil-based TMP (trimethylolpropane) ester as an engine lubricant. *Energy* **2013**, *54*, 167–173. [[CrossRef](#)]
53. Shahabuddin, M.; Masjuki, H.H.; Kalam, M.A.; Bhuiya, M.M.K.; Mehat, H. Comparative tribological investigation of bio-lubricant formulated from a non-edible oil source (*Jatropha* oil). *Ind. Crops Prod.* **2013**, *47*, 323–330. [[CrossRef](#)]
54. Syahrullail, S.; Izhan, M.I.; Rafiq, A.K.M. Tribological investigation of RBD palm olein in different sliding speeds using pin-on-disk tribotester. *Sci. Iran. Trans. B Mech. Eng.* **2014**, *21*, 162–170.
55. Mungse, H.P.; Khatri, O.P. Chemical functionalized reduced graphene oxide as a novel material for reduction of friction and wear. *J. Phys. Chem. C* **2014**, *118*, 14394–14402. [[CrossRef](#)]
56. Ahammed, N.; Asirvatham, L.G.; Wongwises, S. Entropy generation analysis of graphene-alumina hybrid nanofluids in multiport minichannel heat exchanger coupled with thermoelectric cooler. *Int. J. Heat Mass Transf.* **2016**, *103*, 1084–1097. [[CrossRef](#)]
57. Sundar, L.S.; Sharma, K.V.; Singh, M.K.; Sousa, A.C.M. Hybrid nanofluids preparation, thermal properties, heat transfer and friction factor—a review. *Renew. Sustain. Energy Rev.* **2017**, *68*, 185–198. [[CrossRef](#)]
58. Peña-Parás, L.; Taha-Tijerina, J.; Garza, L.; Maldonado-Cortés, D.; Michalczewski, R.; Lapray, C. Effect of CuO and Al<sub>2</sub>O<sub>3</sub> nanoparticle additives on the tribological behaviour of fully formulated oils. *Wear* **2015**, *332–333*, 1256–1261. [[CrossRef](#)]
59. Garg, J.; Poudel, B.; Chiesa, M.; Gordon, J.B.; Ma, J.J.; Wang, J.B.; Ren, Z.F.; Kang, Y.T.; Ohtani, H.; Nanda, J.; et al. Enhanced thermal conductivity and viscosity of copper nanoparticles in ethylene glycol nanofluid. *J. Appl. Phys.* **2008**, *103*, 074301. [[CrossRef](#)]